Japanese Journal of Applied Physics **60**, 072004 (2021).https://doi.org/10.35848/1347-4065/ac06b6

A tunable acoustic filter using disordered systems

Norihiko Nishiguch*

Faculty of Engineering, Division of Applied Physics,

Hokkaido University, Sapporo 060-8628, Japan

Tatsuya Yoshihiro

Graduate School of Engineering, Department of Applied Physics,

Hokkaido University, Sapporo 060-8628, Japan

(Dated: Received March 2, 2021; revised May 25, 2021; accepted May 31, 2021; published online June 18, 2021)

Abstract

We propose a tunable acoustic filter using superlattices constructed by random stacking of solid and fluid layers. Acoustic waves are localized in the random superlattices and the transmission rates substantially decay to 0 except for the resonance transmissions where the acoustic waves are delocalized. The transmission rates become unity for the resonance transmissions. The resonance frequencies depend on the layer thicknesses, and we can modulate the transmission spectra from transparent to opaque, and vice versa, modifying the layer thicknesses. We numerically illustrate the changes in the transport properties for the aluminum/water random superlattices, and suggest to exploit the random superlattices for the tunable acoustic filters.

I. INTRODUCTION

Artificial materials containing a variety of periodic arrays of scatterers for optical and acoustic waves referred to as photonic[1–7] and phononic crystals[8–24] have attracted much attention for decades. They can prohibit and allow the wave propagations and also confine the waves, which is expected to lead to a wide range of applications. The primary interests are the states of waves in the periodic structures, i.e. the band structures and corresponding eigenvectors, and transmission properties. A key property of the band structures is the width of the band gaps. Wide band gaps are useful for insulating and/or confining waves and also helpful for manipulating propagations of wave packets. In particular, the very wide band gaps are helpful for blocking noises of various frequencies in the environment. Another important property is the pass band width of waves. Very narrow pass bands will be helpful for selective transmission of waves with high resolution. If we could tune the band gaps and the pass bands, the system will be a very useful device for controlling waves.

The band gaps are owing to the Bragg diffraction. A suitable choice of structural parameters will realize some wide band gaps, but the band gaps and pass bands appear alternately with increasing frequency for the periodic structures. Inevitably the performance of the periodic systems will be limited as for the blocking the environmental noises. If the device could let waves with only a particular frequency pass and reflect waves of other frequencies, the device will exhibit the substantial performance as a filter without suffering from the

* Norihiko Nishiguch:nn@eng.hokudai.ac.jp

noises. As a candidate of such a system, we think of disordered systems.

It is known that the interference among waves scattered in disordered media causes weak localization phenomena referred to as Anderson localization[25, 26]. The phenomena occur not only for quantum waves but also for classical waves like optical and acoustic waves[27–38]. The localization phenomena are apt to occur for low dimensions, and all the states are localized in the one and two-dimensional systems[26]. One of the simplest disordered structures is a random superlattice(RSL) which is constructed by stacking two layers of dissimilar materials at random. In the previous works[34, 35], we theoretically examined phonon propagations in the RSL's composed of GaAs and AlAs layers. The average transmission rates $\langle T \rangle$ of the GaAs/AlAs RSL's show approximately exponential decays with respect to propagating distance in the wide frequency region owing to Anderson localization except for resonance transmissions. The resonance transmissions occur when the thicknesses of layers are equal to an integer multiple of half wavelength of phonons. Phonons of the wavelength are not scattered at the interfaces, so that phonons are delocalized and then the transmission rates become unity or almost unity, depending on the materials of the substrate and detector. Since the delocalization takes place at around the resonance frequencies, the transmission rates show sharp peaks with respect to frequency. The resonance frequencies are tunable since they are related to the layer thickness. Hence, taking advantage of Anderson localization and delocalization of phonons, we will be able to control the phonon propagations.

Although the GaAs/AlAs RSL's show the transmission decays in the wide frequency regions, the characteristic decay lengths come to 300 layers or more. Then the system size becomes large in order to get transmission decays enough to suppress the wave propagations. It is necessary to increase the scattering intensities of waves at the interfaces in order to make the decay lengths short. The scattering intensities depend on the difference in acoustic impedances of the constituent materials. The ratio of acoustic impedances of GaAs and AlAs $Z_{\mathrm{GaAs}}/Z_{\mathrm{AlAs}} = 1.20$ and the reflectance is $R = \left|\frac{Z_{\mathrm{GaAs}}-Z_{\mathrm{AlAs}}}{Z_{\mathrm{GaAs}}+Z_{\mathrm{AlAs}}}\right|^2 = 0.088$. As a combination of composing materials having substantially different acoustic impedances, we think of a combination of light metal and fluid, e.g. aluminum and water which has the reflectance $R = 0.842$ at the Al/water interfaces. Then the characteristic decay length is expected to be much shorter than GaAs/AlAs RSL's and then the compact devices for controlling acoustic waves will be feasible. Considering the Al layers are moveable in water, the Al/water RSL's will be a tunable device for acoustic waves. In this work, we investigate the transmission properties of acoustic waves in the Al/water RSL's, and suggest the feasible device structures to control acoustic wave propagations without suffering from noises in the environment.

The plan of this work is as follows; we model the RSL's consisting of solid and fluid layers in § II and formulate the transmission rates using a transfer matrix theory. We illustrate the average transmission rates and transmission fluctuations relevant to Anderson localization for Al/water RSL's in § III. We also examine anomalous transmission fluctuations independent of Anderson localization. In § IV, we discuss methods to tune the frequency widows for wave transmissions and to reflect waves in the entire frequency region. A conclusion is given in § V.

II. MODEL AND FORMALISM

A. Model

We consider a RSL which is constructed by stacking solid and fluid layers at random with prescribed probabilities as shown in Fig. 1. The total number of layers is N, and the thickness of k th layer is designated by d_k. The RSL is put between solid substrate (S) and detector (D). We take the x axis to be normal to the interface between the substrate and RSL, and the put the origin at the interface.

B. Elastic wave propagation in solid layers

The equation of motion of displacement vector $\mathbf{u}$ in an isotropic material of mass density ρ_S is given by[39]

$$\rho_S \frac{\partial^2}{\partial t^2}\mathbf{u} = (\lambda + \mu)\nabla\nabla \cdot \mathbf{u} + \mu\nabla^2\mathbf{u}, \tag{1}$$

where λ and μ are the Lamé parameters. The displacement vector $\mathbf{u}$ is composed of longitudinal and transverse waves. Considering that the waves impinge normally on the RSL surface from the substrate, the transverse waves are perfectly reflected at the first interface between the solid and fluid layers, and only the longitudinal acoustic waves are transmitted in the RSL's. Devoting ourselves to the longitudinal waves, we have the following equation

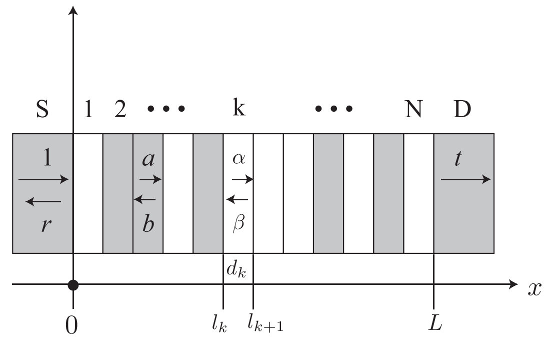

FIG. 1. A random superlattice is modeled by random stacking of solid(shaded regions) and fluid(open regions) layers. d_k is the thickness of k th layer, and the total number of layers is N. L is the size of the random superlattice. a and b (α and β) mean the amplitude of longitudinal waves (pressure waves) traveling forward and backward in solid (fluid) layers. S and D mean the substrate and detector, and r and t are the amplitudes of reflected and transmitted waves.

of motion

$$\left(\frac{1}{c_S^2}\frac{\partial^2}{\partial t^2} - \frac{\partial^2}{\partial x^2}\right) u_S = 0, \tag{2}$$

where u_S is the displacement of longitudinal waves traveling in the x direction and c_S is its sound velocity $c_S = \sqrt{(\lambda + 2\mu)/\rho_S}$. Assuming a plane wave, the displacement u_S yields

$$u_S = (ae^{iq_S x} - be^{-iq_S x})e^{-i\omega t}, \tag{3}$$

where q_S and ω are the wavenumber and angular frequency. The coefficients a and b are the amplitudes of waves traveling forward and backward in the x direction. Putting Eq. (3) into (2), we have the linear dispersion relation

$$\omega = c_S q_S. \tag{4}$$

Using Eq. (3), we obtain the stress tensor element σ_{xX} for the x direction on the X surface

$$\sigma_{xX} = (\lambda + 2\mu) i q_S (ae^{iq_S x} + be^{-iq_S x})e^{-i\omega t}. \tag{5}$$

For convenience, we introduce the following vector $\mathbf{V}_S$ composed of the particle velocity $v_S = -i\omega u_S$ and the stress tensor

$$\mathbf{V}_S(x) \equiv \begin{pmatrix} v_S \\ -\frac{\sigma_{xX}}{Z_F} \end{pmatrix} = -i\omega \Lambda_S E_S(x) \begin{pmatrix} a \\ b \end{pmatrix} e^{-i\omega t}, \tag{6}$$

where

$$\Lambda_S \equiv \begin{pmatrix} 1 & -1 \\ \frac{Z_S}{Z_F} & \frac{Z_S}{Z_F} \end{pmatrix} \tag{7}$$

and

$$E_S(x) \equiv \begin{pmatrix} e^{iq_S x} & \\ & e^{-iq_S x} \end{pmatrix}. \tag{8}$$

Z_S and Z_F are the acoustic impedance of solid $Z_S = (\lambda + 2\mu)/c_S = \rho_S c_S$ and that of fluid $Z_F = \rho_F c_F$ where ρ_F and c_F are the mass density of fluid and the sound velocity in fluid. It is found from Eq. (6) that $\mathbf{V}_S$'s separated by Δx are related using a transfer matrix $\mathcal{S}$ as

$$\mathbf{V}_S(x + \Delta x) = \mathcal{S}(\Delta x)\mathbf{V}_S(x). \tag{9}$$

The transfer matrix $\mathcal{S}$ is defined by

$$\begin{aligned} \mathcal{S}(\Delta x) &\equiv \Lambda_S E_S(\Delta x)\Lambda_S^{-1} \\ &= \begin{pmatrix} \cos(q_S\,\Delta\,x) & i\frac{Z_F}{Z_S}\sin(q_S\,\Delta\,x) \\ i\frac{Z_S}{Z_F}\sin(q_S\,\Delta\,x) & \cos(q_S\,\Delta\,x) \end{pmatrix}, \end{aligned} \tag{10}$$

which has the following properties;

$$|\mathcal{S}| = 1 \tag{11}$$

$$\mathcal{S}(x)\mathcal{S}(y) = \mathcal{S}(x + y) \tag{12}$$

$$\mathcal{S}(\Delta x)^n = \mathcal{S}(n\Delta x). \tag{13}$$

C. Pressure waves in fluid

Considering an ideal fluid under an adiabatic approximation, the velocity of fluid particle $\mathbf{v}_F$ and the pressure P measured from the static pressure P_0 can be expressed using a potential function Ψ[40] as

$$\mathbf{v}_F = -\nabla\Psi \tag{14}$$

and

$$P = \rho_F \frac{\partial}{\partial t}\Psi. \tag{15}$$

The potential Ψ obeys a wave equation that is derived from the continuity equation and the Navier-Stokes equations for fluid as

$$\frac{1}{c_F^2}\frac{\partial^2\Psi}{\partial t^2} - \nabla^2\Psi = 0. \tag{16}$$

Supposing that the waves travel in the x direction, we have

$$\Psi = c_F(\alpha e^{iq_F x} + \beta e^{-iq_F x})e^{-i\omega t}, \tag{17}$$

where q_F is the wavenumber, and α and β are the amplitudes of potential waves traveling forward and backward. Putting Eq. (17) into Eqs. (14), (15) and(16), we obtain the velocity of fluid particle and pressure

$$v_F = -i\omega(\alpha e^{iq_F x} - \beta e^{-iq_F x})e^{-i\omega t} \tag{18}$$

$$P = -i\omega Z_F(\alpha e^{iq_F x} + \beta e^{-iq_F x})e^{-i\omega t} \tag{19}$$

and the linear dispersion relation of waves in fluid

$$\omega = c_F q_F. \tag{20}$$

Here we introduce the vector $\mathbf{V}_F$ composed of v_F and P as the counterpart of $\mathbf{V}_S$

$$\mathbf{V}_F(x) \equiv \begin{pmatrix} v_F \\ \frac{P}{Z_F} \end{pmatrix} = -i\omega\Lambda_F E_F(x)\begin{pmatrix} \alpha \\ \beta \end{pmatrix} e^{-i\omega t} \tag{21}$$

where

$$\Lambda_F \equiv \begin{pmatrix} 1 & -1 \\ 1 & 1 \end{pmatrix} \tag{22}$$

$$E_F(x) \equiv \begin{pmatrix} e^{iq_F x} & \\ & e^{-iq_F x} \end{pmatrix}. \tag{23}$$

$\mathbf{V}_F$'s separated by Δx are related by a transfer matrix $\mathcal{F}(\Delta x)$

$$\mathbf{V}_F(x + \Delta x) = \mathcal{F}(\Delta x)\mathbf{V}_F(x). \tag{24}$$

The transfer matrix $\mathcal{F}(\Delta x)$ is defined by

$$\begin{aligned} \mathcal{F}(\Delta x) &\equiv \Lambda_F E_F(\Delta x)\Lambda_F^{-1} \\ &= \begin{pmatrix} \cos(q_F\Delta x) & i\sin(q_F\Delta x) \\ i\sin(q_F\Delta x) & \cos(q_F\Delta x) \end{pmatrix}, \end{aligned} \tag{25}$$

which exhibits the relations corresponding to Eqs. (11), (12) and (13) about $\mathcal{S}$ as follows;

$$|\mathcal{F}| = 1 \tag{26}$$

$$\mathcal{F}(x)\mathcal{F}(y) = \mathcal{F}(x+y) \tag{27}$$

$$\mathcal{F}(\Delta x)^n = \mathcal{F}(n\Delta x). \tag{28}$$

D. Transmission rates

The transfer matrices $\mathcal{S}$ and $\mathcal{F}$ express the propagation of $\mathbf{V}_S$ and $\mathbf{V}_F$ in solid and fluid layers. Considering that $\mathbf{V}_S$ and $\mathbf{V}_F$ coincide at the interfaces between the solid and fluid layers, the vector $\mathbf{V}_S(L)$ at the interface between the RSL and detector is given by the successive products of $\mathcal{S}$ or $\mathcal{F}$ corresponding to the materials of each layer and $\mathbf{V}_S(0)$ at the interface between the RSL and substrate

$$\mathbf{V}_S(L) = \prod_{k=1}^{N} U_k(d_k)\mathbf{V}_S(0) \tag{29}$$

$$= \begin{pmatrix} R_{11} & R_{12} \\ R_{21} & R_{22} \end{pmatrix} \mathbf{V}_S(0), \tag{30}$$

where U_k means

$$U_k(d_k) = \mathcal{S}(d_k) \text{ or } \mathcal{F}(d_k), \tag{31}$$

and $\{R_{ij}\}$ is the 2×2 matrix that arises from the products of matrices U_k.

Putting $a = 1$ and $b = r$ in $\mathbf{V}_S(0)$ and $a = t$ and $b = 0$ in $\mathbf{V}_S(L)$, we obtain the amplitudes r and t as

$$r = \frac{R_{11} - R_{22} + (Z_S/Z_F)R_{12} - (Z_F/Z_S)R_{21}}{R_{11} + R_{22} - (Z_S/Z_F)R_{12} - (Z_F/Z_S)R_{21}} \tag{32}$$

$$t = \frac{2\, e^{-iq_S L}}{R_{11} + R_{22} - (Z_S/Z_F)R_{12} - (Z_F/Z_S)R_{21}}. \tag{33}$$

Here we use $\det R = \prod_k |U_k| = 1$ from Eqs. (11) and (26) for derivation of the amplitudes. The resultant transmission rate T yields

$$T = |t|^2 = \left| \frac{2}{R_{11} + R_{22} - (Z_S/Z_F)R_{12} - (Z_F/Z_S)R_{21}} \right|^2. \tag{34}$$

III. TRANSMISSION PROPERTIES

A. Average Transmission rates

We first examine the transmission rates of RSL's consisting of Al and water layers whose thicknesses are $d_{\rm S} = d_{\rm F} = 1$ mm. The sound velocity in water $c_F = 1479.9$m/s at 20°C and the sound velocity in Al $c_S = 3.197 \times 10^5$ m/s. The layers are randomly stacked with the same probabilities 1/2. Since the transmission rates depend on the configurations of layers, we investigate the average transmission rates $\langle T \rangle$ over 1000 different configurations of layers.

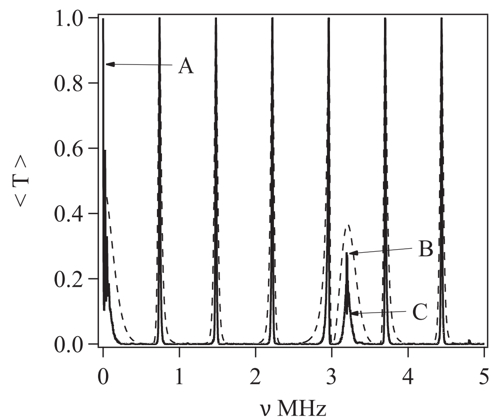

FIG. 2. Average transmission rate $\langle T \rangle$ versus frequency ν of acoustic waves in Al/water RSL's with $N = 30$. Transmission properties of data points referred to as A, B and C at $\nu_A = 0.001$MHz, $\nu_B = 3.194$MHz and $\nu_C = 3.197$MHz will be examined in detail. The dashed line indicates the average transmission rates derived analytically by means of Green's function[34].

Figure 2 plots $\langle T \rangle$ versus frequency ν of the Al/water RSL's with $N = 30$. The transmission rates are averaged over 1000 different configurations of layers. There are present two kinds of sharp peaks with $\langle T \rangle = 1$ and $\langle T \rangle \approx 0.3$. The full width at half maximum (FWHM) of the primary peaks with $\langle T \rangle = 1$ is $\Delta\nu = 0.015$MNz. On the other hand, $\langle T \rangle$ oscillates rapidly between (B) 0.28 and (C) 0.09 with respect to frequency around the secondary peak labeled B although it is not clearly shown in Fig. 2. Aside from the peaks, $\langle T \rangle$ decays and almost vanishes owing to Anderson localization.

Before proceeding the discussions, we note the difference in the localized states between Anderson localization and the forbidden bands in the periodic superlattice (PSL). Figure 3 exhibits the spatial distribution of amplitudes $\sqrt{\langle \rho v^2 \rangle}$ of acoustic waves at 2MHz averaged over 1000 RSL's with $N = 30$ as well as the amplitudes of acoustic waves at the same frequency in the Al/water PSL with $N = 30$. The thicknesses of constituent layers of the PSL are the same as those of the RSL's. The frequency is contained within one of the band gaps in the PSL, and then both the amplitudes decay exponentially with respect to the distance from the substrate. The decay length l defined by $l^{-1} = -\frac{d}{dx} \log \sqrt{\langle \rho v^2 \rangle}$ is $l_{PSL} = 2.09$mm for the PSL and $l_{RSL} = 4.36$mm for the RSL's. l_{RSL} is larger than twice as large as l_{PSL}, indicating that Anderson localization is weak localization in contrast to the localized states in the forbidden band in the PSL.

Using the decay length, the transmission rates of RSL's with N layers are approximately estimated by $e^{-2Nd/l_{RSL}} \sim e^{-0.46N}$. The magnitude becomes $e^{-13.8} \approx 1 \times 10^{-6}$ for $N = 30$, indicating the transmission rate small enough to reflect the acoustic waves. For $N = 20$, it becomes approximately 1×10^{-4}. As for the RSL's smaller than $N = 20$, the average transmission rates increase in the entire frequency region. These approximated values agree with the numerical data of $\langle T \rangle$. Thus the decrease in size of the RSL's increases the average transmission rates. The increase in the transmission rates simultaneously gives rise to the increase in the FWHM of the transmission peaks. For example, the FWHM of the transmission peaks becomes $\Delta\nu = 0.02$MNz for $N = 20$. Considering the sharp pass bands and blocking the acoustic waves of other frequencies, we investigate the transmission properties in the RSL's with $N = 30$ in the rest of this work.

The transmission peaks are owing to the respective resonance transmissions in the Al and water layers. When the phase development of waves traveling in a water layer is equivalent to π multiplied by an integer n, i.e. $q_F d_F = \frac{2\pi\nu d_F}{c_F} = n\pi$, the transfer matrix $\mathcal{F}(d_F)$ becomes the 2×2 identity matrix multiplied by the phase factor $e^{in\pi} = (-1)^n$, and then the matrix R depends only on the products of $\mathcal{S}(d_k)$'s. In other words, the RSL is regarded as composed effectively of only the Al layers. Because the water layers are regarded as absent in the system, the amplitudes of reflection r and transmission t become $r = 0$ and $t = e^{i\phi}$, where $e^{i\phi}$ is the phase factor which depends on the number of Al layers, so that $T = 1$. The resonance frequencies $\nu_{F,n}$ are derived from the phase development as $\nu_{F,n} = \frac{nc_F}{2d_F} = 0.740 \times n\,\mathrm{MHz}(\mathrm{n} = 1, 2, \ldots)$, which coincide with the transmission peak frequencies.

On the other hand, the secondary peak labeled B is owing to the resonance transmissions

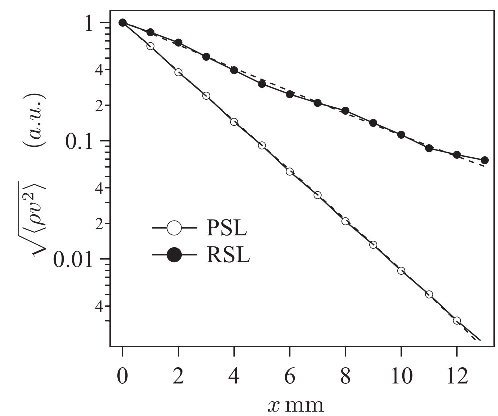

FIG. 3. Amplitudes of velocity in the Al/water periodic superlattice(PSL) with $N = 30$ at $\nu =$ 2MHz in the band gap versus the distance from the substrate together with the averaged amplitudes in the Al/water RSL's with the same size. The decay length l is $l_{PSL} = 2.09$mm for the Al/water PSL and $l_{RSL} = 4.36$mm for the Al/water RSL's.

in Al layers. The resonance frequencies $\nu_{S,n}$ are evaluated to be $\nu_{S,n} = 3.197 \times n\,\mathrm{MHz}(\mathrm{n} = 1, 2, \ldots)$, and $\nu_{S,1}$ agrees with the frequency of the secondary peak. At the resonance frequencies, $\mathcal{S}(d_S)$ becomes the 2×2 identity matrix multiplied by $e^{in\pi}$. Since the Al layers between water layers are regarded as absent, the RSL can be treated as a large single water layer. Considering the acoustic waves are reflected only at the surfaces of the substrate and the detector, we obtain the transmission rate through the single water layer as

$$T_R(n_F d_F) = \frac{1}{1 + \frac{1}{4}\left(\frac{Z_S}{Z_F} - \frac{Z_F}{Z_S}\right)^2 \sin^2(q_F n_F d_F)}. \tag{35}$$

In Eq. (35), n_F is the total number of water layers which depends on the RSL's. Introducing the following probability $P_N(n_F)$ that a RSL made of N layers contains n_F water layers

$$P_N(n_F) = \frac{{}_N C_{n_F}}{2^N}, \tag{36}$$

the average transmission rate $\langle T_R \rangle$ yields

$$\langle T_R \rangle = \sum_{n_F=0}^{N} P_N(n_F) T_R(n_F d_F). \tag{37}$$

At $\nu_{S,1}$, we have $\langle T_R \rangle = 0.09$, which agrees with $\langle T \rangle$ labeled C at the center of the secondary peak in Fig. 2. $\langle T_R \rangle$ oscillates in the narrow frequency region around the resonance frequency and reaches to $\langle T \rangle$ labeled B. Thus the width of oscillating $\langle T_R \rangle$ is comparable to that of $\langle T \rangle$. This accounts for the oscillations of $\langle T \rangle$ around the secondary peak of $\langle T \rangle$.

The dashed line in Fig. 2 shows $\langle T \rangle$ versus ν based on the theory that assumes weak scattering at the interfaces[34, 35]. Although the frequency dependence of the theory agrees with the numerical data, the theory overestimates $\langle T \rangle$. The theory will need to incorporate the back-scattering processes beyond the weak scattering approximation for the Al/water RSL's. Then in the rest of this work, we will investigate the transmission properties, relying on the numerical data.

B. Transmission fluctuations

As mentioned above, the wave propagations in the RSL's are affected by the interference among waves scattered from the random structures, causing the transmission fluctuations intrinsic to Anderson localization. The fluctuations defined by $\Delta T = \sqrt{\langle T^2 \rangle - \langle T \rangle^2}$ depend only on $\langle T \rangle$, and the relation between ΔT and $\langle T \rangle$ is analytically proved to be a universal relation between them, independent of types of randomness[34, 35, 41].

Figure 4 shows ΔT versus $\langle T \rangle$, where the open circles denote the numerical results and the thick solid line like an arc is the theoretical curve[34] intrinsic to Anderson localization. Most the data points agree with the theoretical curve. However, some data points obviously look unrelated to the theoretical curve. A remarkable deviation of ΔT from the theoretical curve is seen for $0.1 < \langle T \rangle < 1$ where ΔT distribute in a loop below the theoretical curve. Another noticeable behavior is found in the region $0.1 < \langle T \rangle < 0.2$ where ΔT distribute across the theoretical curve. Three data points that represent the anomalous behaviors of ΔT are labeled A, B and C in Fig. 4, and the corresponding $\langle T \rangle$ are labeled with the same letters in Fig. 2. The data point A is very close to $\nu = 0$ and then the matrix $\mathcal{S}$ becomes approximately the identity matrix like the data points B and C, indicating the anomalous transmission fluctuations are related to the resonance transmission in Al layers.

Because the anomalous behavior of transmission fluctuations have not been observed in the GaAs/AlAs RSL's, the phenomena are peculiar to the Al/water RSL's under study. It is necessary to clarify the mechanism of the phenomena for full understanding of the transmission properties in the Al/water RSL's. As discussed above, the total water layer thickness $n_F d_F$ is variant, which affects $\langle T \rangle$ for the resonance transmissions in Al layers as

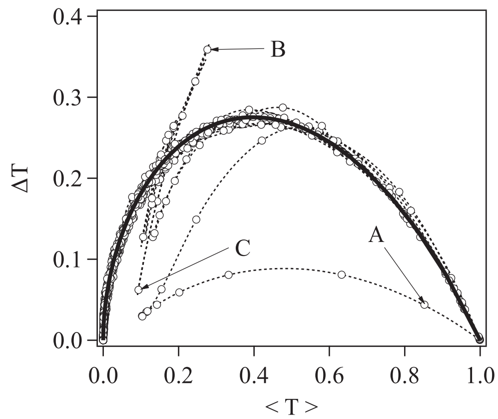

FIG. 4. The transmission fluctuations ΔT versus $\langle T \rangle$ for the Al/water RSL's examined in Fig. 2. The open circles are the numerical data and the solid line indicates the theoretical relationship[34] between ΔT versus $\langle T \rangle$. A, B, and C indicate ΔT at the points designated in Fig. 2.

shown in Eq. (37). The transmission fluctuations ΔT_R caused by the varying total water layer thickness are obtained using the probability (36) as

$$\Delta T_R = \left[\sum_{n_S=0}^{N} P_N(n_S) \left[T_R(n_S d_S) \right]^2 - \langle T_R \rangle^2 \right]^{\frac{1}{2}} . \tag{38}$$

Varying frequency in the regions $0 < \nu < 0.02$MHz and $\nu_{S,1} - 0.02$MHz $< \nu < \nu_{S,1} + 0.02$MHz, we plot ΔT_R versus $\langle T_R \rangle$ in Fig. 5 together with the numerical data (gray open circles) shown in Fig. 4. The dashed line starting from $\Delta T = 0$ at $\langle T \rangle = 1$ is obtained for the frequency region $0 < \nu < 0.02$MHz, showing excellent agreement with the numerical data containing the point A. In contrast to the actual data, the dashed line does neither distribute in loop nor merge into the theoretical curve because the phase development in the Al layers is ignored in Eq. (38). The numerical data crossing the theoretical curves at $\Delta T \approx 0.23$ and $\langle T \rangle \approx 0.2$ are also reproduced by Eq. (38) for the frequency region containing $\nu_{S,1}$, showing quantitative agreement with the numerical data. From the agreement of ΔT_R with ΔT, we confirm that the anomalous transmission fluctuations arise from the uncertain total thickness of water layers for the resonance transmissions in Al layers.

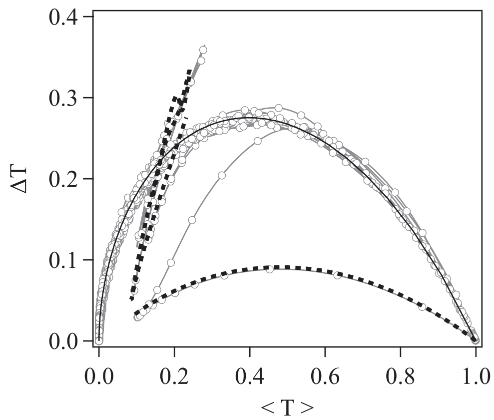

FIG. 5. The transmission fluctuations ΔT versus $\langle T \rangle$ for the resonance transmissions in the Al/water RSL's together with the numerical data (gray open circles) shown in Fig. 4. The dashed lines indicate ΔT_R obtained from Eq. (38), showing excellent agreement with the numerical data ΔT.

IV. TUNING TRANSMISSION RATES

The average transmission rates are $\langle T \rangle = 1$ for the resonance transmissions in water layers and the corresponding fluctuations are $\Delta T = 0$. Thanks to $\Delta T = 0$, all the RSL's exhibit $T = 1$ at the resonance frequencies $\nu_{F,n}$ regardless of the layer configurations. This is the case for $\langle T \rangle = 0$. Since $\Delta T = 0$, all the RSL's exhibit $T = 0$. In contrast, $\langle T \rangle = 0.3$ for the resonance transmissions in Al layers and $\Delta T \approx \langle T \rangle$ as shown in Fig. 4. The relation $\Delta T \approx \langle T \rangle$ leads to substantial sample dependence of the transmission rates. Considering that the devices should be free from the sample-dependent characteristics, we will suppress the resonance transmissions in Al layers.

Here we introduce obstacles for wave propagations working at the resonance frequencies $\nu_{S,n}$. The obstacles are the Al layers whose thickness is the original thickness multiplied by an irrational number. Because of the difference in layer thicknesses, the original and new Al layers do not have common resonance frequencies. As a result, the resonance transmissions in Al layers will vanish and only the resonance transmissions in the water layers will take place in the RSL's.

Fugue 6 shows $\langle T \rangle$ versus ν for the Al/water RSL's consisting of the water and two kinds of Al layers. The thicknesses of the water layers are $d_F = 1$mm, and those of the two kinds of Al layers are $d_{S_1} = 1$mm and $d_{S_2} = \sqrt{2}$mm. The probabilities of appearance of the two Al layers are 1/4 for each kind of layers and that for the water layers is 1/2. The total number of layers is $N = 30$ and the transmission rates are averaged over 1000 ensembles. The resonance transmissions in Al layers are obviously suppressed as expected, and then we

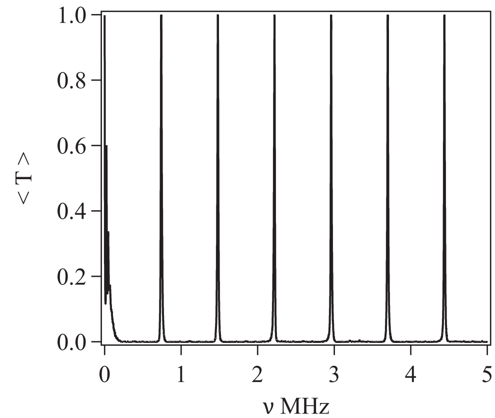

FIG. 6. Average transmission rate $\langle T \rangle$ versus frequency ν for the Al/water RSL's consisting of the water layer of $d_F = 1$mm thick and two kinds of Al layers of $d_{S_1} = 1$mm and $d_{S_2} = \sqrt{2}$mm thick. The appearance probabilities of the two Al layers are 1/4 and that for the water layers is 1/2. The total number of layers is $N = 30$ and the transmission rates are averaged over 1000 ensembles.

have only the primary peaks due to the resonance transmissions in water layers.

Using the same method, it is possible to select a transmission channel out of the primary peaks. We further introduce the water layers whose thickness d_{F_2} is the original thickness d_{F_1} multiplied by a rational number. The resonance frequencies are $\nu_{F,n} = nc_F/2d_{F_1}$ for the original water layers, and those of new layers are $\nu'_{F,n'} = n'c_F/2d_{F_2}$. These frequencies do not match except when $\nu_{F,n}$ and $\nu'_{F,n'}$ are a common multiple of $c_F/2d_{F_2}$ and $c_F/2d_{F_2}$. Then the resonance transmissions through both the water layers will occur only at the frequencies $\nu_{F,n} = \nu'_{F,n'}$. Figure 7 shows $\langle T \rangle$ versus ν of the RSL's which consist of the Al layers with $d_{S_1} = 1$mm and $d_{S_2} = \sqrt{2}$mm thick and the water layers with $d_{F_1} = 1$mm and $d_{F_2} = 1.4$mm thick. The four layers are randomly stacked at the same probabilities 1/4. The least common multiple of $\nu_{F,n}$ and $\nu'_{F,n'}$ is $\nu_{F,5} = \nu'_{F,7} = 3.7$MHz. Figure 7 exhibits only the transmission peak at the frequency and other transmission peaks disappear as expected.

When all the layers do not have a common frequency for resonance transmissions, all the waves will be localized and exhibit substantial decays of transmission rates. Figure 8

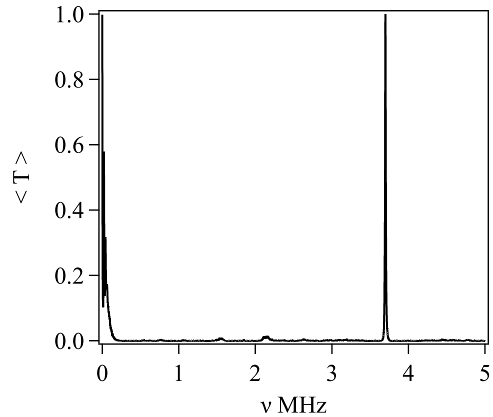

FIG. 7. Average transmission rate $\langle T \rangle$ versus frequency ν for random superlattices made of a solid layer of $d_S = 1$mm thick and two fluid layers of $d_{F_1} = 1$mm, $d_{F_2} = 1.4$mm thick. The number of layers is $N = 30$ and the transmission rates are averaged over 1000 ensembles. Only the transmission peak at $\nu = 3.7$MHz appears and other peaks due to resonance transmissions are dismissed.

shows $\langle T \rangle$ versus ν for the RSL's consisting of three different fluid layers with $d_{F_1} = 1$mm, $d_{F_2} = \sqrt{2}$mm and $d_{F_3} = \sqrt{3}$mm thick, and two different solid unit layers with $d_{S_1} = 1$mm and $d_{S_2} = \sqrt{2}$mm thick. The layers are stacked randomly at equal probabilities 1/6 for water layers and 1/4 for Al layers. The average transmission rates are very close to 0 in the entire frequency region except for the very low frequency region since the acoustic waves are extended in the frequency region for the finite system size.

V. CONCLUSION

In the present work, we suggest the tunable acoustic filters using the Al/water RSL's. The acoustic waves are intrinsically localized in the RSL's in the entire frequency region due to Anderson localization, and the transmission rates vanish except for the resonance transmissions. The resonance transmissions occur when the thicknesses of layers are equal to an integer multiple of half wavelength of waves, and the acoustic waves are extended and the transmission rates are unity. Paying special attention to that the resonance transmissions depend on the layer thickness, we investigated tuning the resonance frequencies as well as designing the transmission spectra from transparent to opaque via changes in the thicknesses

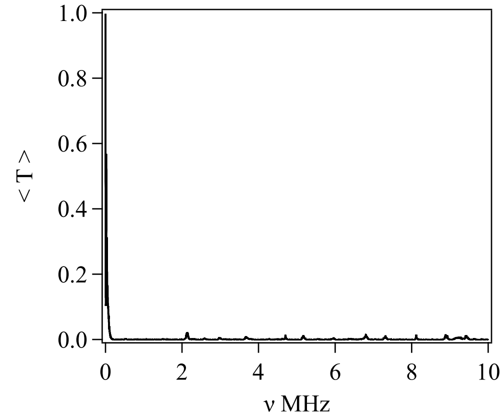

FIG. 8. Average transmission rate $\langle T \rangle$ versus frequency ν for random superlattices made of two solid layer of $d_{S_1} = 1$mm, $d_{S_2} = \sqrt{2}$mm thick and three fluid layers of $d_{F_1} = 1$mm, $d_{F_2} = \sqrt{2}$mm and $d_{F_3} = \sqrt{3}$mm thick. Because there is no resonance frequency in both solid and water layers, there is no prominent transmission peaks.

of constituent layers. We numerically illustrated the changes in the transmission spectra for the Al/water RSL's for four different cases of constituent layers as shown in Figs. 2, 6, 7 and 8. The water layer thickness can be adjusted by moving the Al layers, and the transmission spectra shown in Figs. 6, 7 and 8 appear in the same device. The findings of the present work will lead to the tunable acoustic filters having the wide band gaps and sharp pass bands.

ACKNOWLEDGMENTS

This work was supported by JSPS KAKENHI Grant Number JP19H02647.

[1] J. D. Joannopoulos,R. D. Meade and J.N. Winn, *Photonic Crystals*, Princeton University Press, Princeton, (1995).

[2] C. M. Soukoulis, *Photonic Band Gap Materials*, Kluwer Academic, Dordrecht (1996).

[3] Z. Y. Li and K. M. Ho, Phys. Rev. B **68**, 155101(2003).

[4] L-M. Li and Z-Q. Zhang, Phys. Rev. B **58**, 9587(1998).

[5] Pendry, J. B., Phys. Rev. Lett. **85**, 3966(2000).

[6] K. Sakoda, *Optical Properties of Photonic Crystals*, Springer-Verlag Berlin Heidelberg, 2nd ed. (2005).

[7] O. Sigmund and K. Hougaard, Phys. Rev. Lett. **100**, 153904(2008).

[8] E. Yablonovitch, Phys. Rev. Lett. **58**, 2059 (1987).

[9] E. N. Economou and M. M. Sigalas, Phys. Rev. B **48**, 13434(1993).

[10] M. S. Kushwaha and P. Halevi, J. Acoust. Soc. Am. **101**, 619(1997).

[11] J. O. Vasseur, P. A. Deymier, B. Chenni, B. Djafari-Rouhani, L. Dobrzynski, and D. Prevost, Phys. Rev. Lett. **86**, 3012(2001).

[12] M. Kafesaki and E. N. Economou, Phys. Rev. B **60**, 11993(1999).

[13] M. S. Kushwaha, P. Halevi, L. Dobrzynski, and B. Djafari-Rouhani, Phys. Rev. Lett. **71**, 2022 (1993).

[14] R. Martínez-Sala, J. Sancho, J. V. Sánchez, V. Gómez, J. Llinares and F. Meseguer , Nature **378**, 241-242(1995) .

[15] M. M. Sigalas and E. N. Economou, J. SoundVib. **158**, 377(1992).

[16] C. Y. Qiu and L. Zhengyou, Appl. Phys. Lett. **89**, 063106 (2006).

[17] J. H. Page, Ping Sheng, H. P. Schriemer, I. Jones, Xiaodun Jing and D. A. Weitz, Science **271**, 634(1996).

[18] H. P. Schriemer, M. L. Cowan, J. H. Page, Ping Sheng, Zhengyou Liu, and D. A. Weitz, Phys. Rev. Lett. **79**, 3166(1997).

[19] X. D. Zhang and Z. Y. Liu, Appl. Phys. Lett. **85**, 341 (2004).

[20] K. Imamura and S. Tamura, Phys. Rev. B **70**, 174308(2004).

[21] A. V. Akimov, Y. Tanaka, A. B. Pevtsov, S. F. Kaplan, V. G. Golubev, S. Tamura, D. R. Yakovlev, and M. Bayer, Phys. Rev. Lett. **101**, 033902(2008).

[22] M. S. Kushwaha, P. Halevi, G. Martínez, L. Dobrzynski, and B. Djafari-Rouhani, Phys. Rev. B **49**, 2313 (1994).

[23] W. Fugen, L. Zhengyou and L. Youyan, J. Phys. D: Appl. Phys. **35** 162-165(2002).

[24] T. Wang, M.-P. Sheng, H. Wang and Q.-H. Qin, Acoustics Australia **43**, 275-281(2015).

[25] P.W. Anderson, Rev. Mod. Phys. **50**,191(1978).

[26] E. Abrahams, P. W. Anderson, D. C. Licciardello and T. V. Ramakrishnam: Phys. Rev. Lett., **42**, 673 (1979) .

[27] K. Ishii, Prog. Theor. Phys. Suppl. 53, 77 (1973).

[28] *Scattering and Localization of Classical Waves in Random Media*, edited by P. Sheng (World Scientific, Singapore, 1990).

[29] S. John, H. Sompolinsky, and M. J. Stephen, Phys. Rev. B **27**, 5592(1983)

[30] T. R. Kirkpatrick, Phys. Rev. B **31**, 5746(1985).

[31] S. John, Phys. Rev. Lett. **53**, 2169(1985).

[32] S. John, Phys. Rev. Lett. **58**, 2486(1987).

[33] S. Tamura and F. Nori, Phys. Rev. B**41**, 7941(1990).

[34] N. Nishiguchi, S. Tamura, and F. Nori, Phys. Rev. B **48**, 2515-2528 (1993).

[35] N. Nishiguchi, S. Tamura, and F. Nori, Phys. Rev. B **48**, 14426-14435 (1993)

[36] T. Yoshihiro and N. Nishiguchi, Phys. Rev. B **100**, 235441(1-10) (2019) .

[37] A. Chaudhuri, A. Kundu, D. Roy, A. Dhar, J. L. Lebowitz, and H. Spohn, Phys. Rev. B **81**, 064301 (2010).

[38] H. A. Fertig and T. L. Reinecke, Phys. Rev. B **50**, 7443-7452(1994).

[39] L.D. Landau, E. M. Lifshitz, L. P. Pitaevskii and A. M. Kosevich *Theory of Elasticity* 3rd ed. (Elsevier, 2012) Chapter I.

[40] L.D. Landau and E. M. Lifshitz, *Fluid Mechanics* (Pergamon Press,1959) Chapter VIII.

[41] A. A. Abrikosov, Solid State Commun. **37**, 997(1981).